



## Natural radioactivity concentrations of $^{226}\text{Ra}$ , $^{232}\text{Th}$ , and $^{40}\text{K}$ in commercial building materials and their lifetime cancer risk assessment in dwellers

Omeje M., Adewoyin O. Olusegun, Emmanuel S. Joel, Ehi-Eromosele C. O, Emenike C. PraiseGod, Usikalu M. R., Akinwumi Sayo A., Zaidi E. & Mohammad A. Saeed

To cite this article: Omeje M., Adewoyin O. Olusegun, Emmanuel S. Joel, Ehi-Eromosele C. O, Emenike C. PraiseGod, Usikalu M. R., Akinwumi Sayo A., Zaidi E. & Mohammad A. Saeed (2018): Natural radioactivity concentrations of  $^{226}\text{Ra}$ ,  $^{232}\text{Th}$ , and  $^{40}\text{K}$  in commercial building materials and their lifetime cancer risk assessment in dwellers, Human and Ecological Risk Assessment: An International Journal, DOI: [10.1080/10807039.2018.1438171](https://doi.org/10.1080/10807039.2018.1438171)

To link to this article: <https://doi.org/10.1080/10807039.2018.1438171>



Published online: 06 Mar 2018.



Submit your article to this journal [↗](#)







View related articles [↗](#)



View Crossmark data [↗](#)



# Natural radioactivity concentrations of $^{226}\text{Ra}$ , $^{232}\text{Th}$ , and $^{40}\text{K}$ in commercial building materials and their lifetime cancer risk assessment in dwellers

Omeje M. <sup>a</sup>, Adewoyin O. Olusegun<sup>a</sup>, Emmanuel S. Joel<sup>a</sup>, Ehi-Eromosele C. O<sup>b</sup>,  
Emenike C. PraiseGod <sup>c</sup>, Usikalu M. R. <sup>a</sup>, Akinwumi Sayo A. <sup>a</sup>, Zaidi E. <sup>d</sup>,  
and Mohammad A. Saeed<sup>e</sup>

<sup>a</sup>Department of Physics, College of Science and Technology, Covenant University, Ota, Ogun State, Nigeria;

<sup>b</sup>Department of Chemistry, College of Science and Technology, Covenant University, Ota, Ogun State, Nigeria;

<sup>c</sup>Department of Civil Engineering, College of Engineering, Covenant University, Ota, Ogun State, Nigeria;

<sup>d</sup>Faculty of Applied Science and Technology, Universiti Tun Hussein Onn Malaysia, Pagoh Campus, Pagoh, Muar, Johor, Malaysia; <sup>e</sup>Division of Science and Technology, University of Education Township, Lahore, Pakistan

## ABSTRACT

Elevated radioactivity levels of  $^{226}\text{Ra}$ ,  $^{232}\text{Th}$ , and  $^{40}\text{K}$  in building materials were measured using gamma-ray spectrometry and their associated lifetime cancer risks were also determined. The mean activity concentrations of  $^{226}\text{Ra}$ ,  $^{232}\text{Th}$ , and  $^{40}\text{K}$  are  $45.72 \pm 0.55$ ,  $65.90 \pm 8.89$ , and  $487.32 \pm 15.20$  Bq kg<sup>-1</sup>, respectively. Statistically, the principal component (PC) analysis indicates that higher loadings were recorded in Principal Component One (PC1) with large contribution from  $^{232}\text{Th}$  and  $^{40}\text{K}$ . The leverage studies indicate that BN Ceramics (BNC) contributes more to the loadings in PC1 followed by Golden Crown Ceramic (GCC) sample and GC. The mean values of 0.399 mSv y<sup>-1</sup> for annual effective dose from the samples surpassed the world's average value of 0.07 mSv y<sup>-1</sup> by a factor of 5.7. The mean gamma index from the measured samples is 0.644, whereas a mean value of 0.271 for alpha index is noted in the samples. The activity utilization index (AUI) from the samples satisfied the AUI < 2, which corresponded with the annual effective dose of < 0.3 mSv y<sup>-1</sup>, except interlock Site 2 and Gomez Spain tiles. Significantly, the mean value of excess lifetime cancer risk of 0.0014 is slightly lower than the world average value of  $0.29 \times 10^{-3}$ .

## ARTICLE HISTORY

Received 9 December 2017

Revised manuscript

accepted 5 February 2018

## KEYWORDS

building materials;  
radioactivity; gamma  
spectroscopy; excess lifetime  
cancer risk; annual effective  
dose; alpha index

## 1. Introduction

Human society has always been exposed on a daily basis to natural radionuclides such as  $^{232}\text{Th}$ ,  $^{226}\text{Ra}$ , and  $^{40}\text{K}$  (Amin and Naji 2013). These radionuclides in the series are headed by  $^{226}\text{Ra}$  ( $^{238}\text{U}$ ) and are relatively less important from a dosimetric point of view (UNSCEAR 1993).

Humans are exposed to natural radiation from external sources, which include natural radionuclides in the earth (series of uranium-238, uranium-235, and thorium-232) and

**CONTACT** Omeje M.  maxwell.omeje@covenantuniversity.edu.ng  Department of Physics, College of Science and Technology, Covenant University, P.M.B 1023, Ota, Ogun State, Nigeria.

Color versions of one or more of the figures in the article can be found online at [www.tandfonline.com/bher](http://www.tandfonline.com/bher).

© 2018 Taylor & Francis Group, LLC

cosmic radiation, and by internal radiation from natural radionuclides incorporated into the body (UNSCEAR 2000). The main routes of radionuclide intake are ingestion through food, water, and inhalation. A particular category of exposure to internal radiation, in which the bronchial epithelium is irradiated by alpha particles from the short-lived progeny of radon, constitutes a major fraction of the exposure from natural sources (UNSCEAR 2000; Sharma *et al.* 2015).

The worldwide average indoor effective dose due to gamma rays from building materials is estimated to be about  $0.4 \text{ mSv y}^{-1}$  (UNSCEAR 2000; Sharma *et al.* 2015). Globally, building materials that contain radioactive nuclides have been used for many decades. As individuals spend more than 80% of their time indoors, the internal and external radiation exposures from building materials create prolonged exposure situations (ICRP 1999). The use of such materials which contain naturally occurring radionuclides for house construction may enhance the natural radiation background to which some population groups are exposed (UNSCEAR 2000). This exposure occurs on a daily basis and the ability of the radionuclides to move rapidly in air allows them to be easily transmitted into the environment in which humans come in contact with (Gupta *et al.* 2009).

In building construction, the existence of this radionuclide in the raw material such as cement, brick, and tiles may lead to undesirable radiation exposure to the public. The major exposure problem is associated with structure that naturally acts as radionuclide-bearing material (Tzortzis and Tsertos 2004). This indoor radiation exposure is due to the presence of these radioactive elements in the building materials (Jwanbot *et al.* 2014; Qureshi *et al.* 2014). Construction materials are derived from both natural sources (*e.g.*, rock and soil) and waste products (*e.g.*, phosphor-gypsum, alumshale, coal, fly ash, oil shale ash, some are minerals and certain slugs) as well as from industry products (*e.g.*, power plants, phosphate fertilizer, and the oil industry (O'Brein 1997)). Although building materials act as sources of radiation to the inhabitants in dwellings, they also shield against outdoor radiation (Akkurt *et al.* 2007).

In Nigeria, the commercial building materials such as cement, bricks, and tiles have been widely used. Most of them are imported from all over the world such as India, China, Italy, UAE, and Spain. However, some others are from the local supplier around Nigeria. As there is a lack of report in risk exposure for all of these building materials, in this article, focus is given to the assessment of radioactivity concentration and radiological risk indices in commercial building materials.

## 2. Methods and materials

### 2.1. Samples collection and preparations

The river sand used for this study was scooped from a nearby river at Igboloye village in Ota, Ogun State, Nigeria. The area falls within the Eastern Dahomey (Benin) basin of southwestern Nigerian that stretches along the continental margin of the Gulf of Guinea. Rocks in the Dahomey basin are Late Cretaceous to Early Tertiary in age (Jones and Hockey 1964; Omatsola and Adegoke 1981; Billman 1992; Olabode 2006). The stratigraphy of the basin has been classified into Abeokuta Group, Imo Group, Oshoshun, Ilaro, and Benin Formations. The Cretaceous Abeokuta Group consists of Ise, Afowo, and Araromi Formations consisting of poorly sorted ferruginized grit, siltstone, and mudstone with shale-clay layers. The geology of the area is presented in Figure 1.

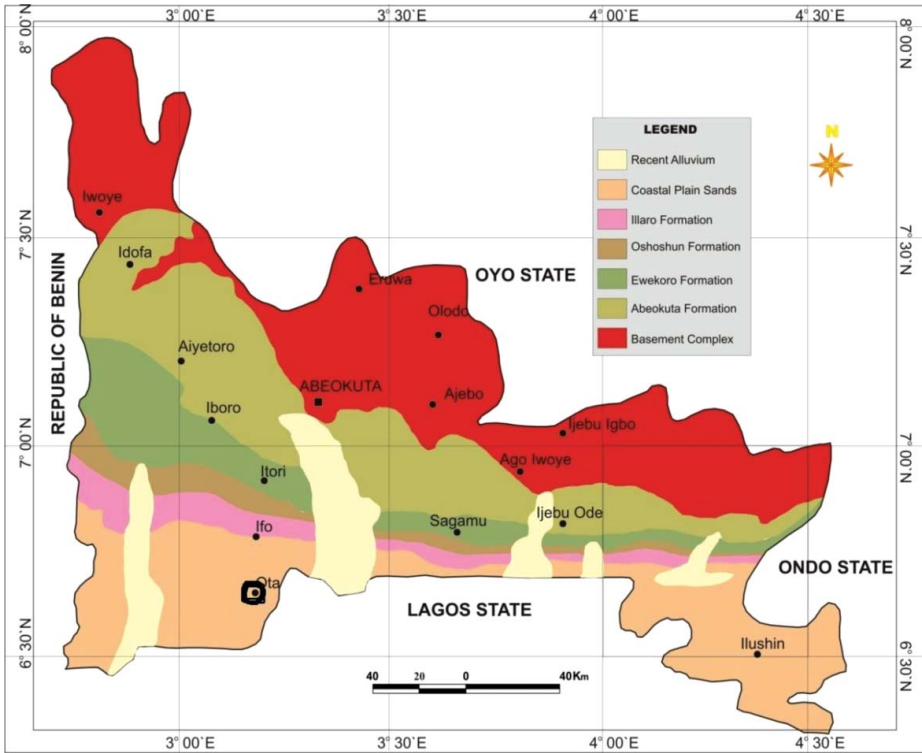


**Figure 1.** Geologic map of Ogun State showing the location where the sand sample was collected (circled in black). Source: Omeje *et al.* (2017).

## 2.2. Samples collection and preparations

The building material samples used for this work were purchased from the Nigerian commercial markets and the river sand was scooped from a nearby river at Igboloye village in Ota, Ogun State, Nigeria. Initial labeling and cataloguing was done for easy identification. The ceramic tiles and the marbles were broken into smaller pieces so as to allow further processing. All the samples were crushed and prepared according to Omeje *et al.* (2013, 2014); and Alnour *et al.* (2012). The sieved samples of ceramic tiles, cement, river channel sand (sharp and plaster), and white cements (two were Nigerian-made and one was from UAE), which were contained in each bottle, weighed 200 g; there was a total of 21 samples in all as listed in Table 1.

## 2.3. Gamma spectroscopy analysis of the radionuclides

The powdered samples were put in a plastic beaker container, sealed for 4 weeks to achieve secular equilibrium (Trimble 1968). Analysis of the samples was conducted in Canada (Activation Analysis Laboratory System) using High-Resolution Germanium detector, Canberra Lynx™ Digital Signal Analyzer (DSA), a 32 K channel integrated signal analyzer and a top-opening lead shield (4" lead, copper/tin liner) to prevent high background counts with 50% relative efficiency and resolution of 2.1 keV at 1.33 MeV gamma energy of  $^{60}\text{Co}$  (Tsoulfanidis 1995). The Genie-2K V3.2 software locates and analyzes the peaks,

**Table 1.** The list of building materials, countries of production, and the sizes.

S/N	Company name	Country of origin	Sample size
1	Black Galaxy India	India	600 × 300 mm
2	Blue Pearl India	India	600 × 300 mm
3	BN Ceramics Floor tiles	Nigeria	450 × 450 mm
4	BN Floor tiles Benia	Spain	600 × 600 mm
5	Dangote Cement (42.5N) Grade	Nigeria	50 kg
6	Elephant Portland Cement	Nigeria	50 kg
7	Golden Crom Floor tiles Ogum	Nigeria	300 × 300mm
8	Golden Crown Ceramics Nig	Nigeria	250 × 400 mm
9	Gomez	Spain	450 × 450 mm
10	Goodwill Ceramics	Nigeria	400 × 250 mm
11	Goodwill verified tile	India	400 × 400 mm
12	Green Pearl India	India	600 × 300 mm
13	Goodwill Super Polish Porcelain tiles	India	600 × 300 mm
14	Iddris Floor tile – China	China	600 × 600 mm
15	Interlock stone tiles Site 3-CU	Nigeria	600 × 600 mm
16	Interlock Stone Site 1	Nigeria	140 × 60 mm
17	Interlock Stone Site 2	Nigeria	140 × 60 mm
18	IRIS Ceramics tiles Italy	Nigeria	250 × 400 mm
19	Golden Crown Floor tiles Ogum	Nigeria	300 × 300 mm
20	Golden Crown Ceramics	China	250 × 400 mm
21	Gomez (Spain) 450 mm	Spain	450 × 450 mm

subtracts background, identifies the nuclides. The efficiency curves for this analysis were corrected for the attenuation and self-absorption effects of the emitted gamma photons. CAMET and IAEA standards (DL-1a, UTS-2, UTS-4, IAEA-372, and IAEA-447) were used for checking the efficiency calibration of the system. For the activity measurements, the samples were counted for 86,400 seconds with the background counts subtracted from the net count. The minimum detectable activity of the detector was determined with a confidence level of 95% (Currie 1968). The uncertainty errors were estimated keeping into account the associated errors from gamma counting emission probability and efficiency calibration standard of the system. The progeny of  $^{226}\text{Ra}$ ,  $^{214}\text{Bi}$ , and  $^{214}\text{Pb}$  emits gamma line 609 keV, 934 keV, 2204 keV, 1764 keV, 351 keV, and 295 keV that were used but the resolution of  $^{226}\text{Ra}$  was from the emission of 1764 keV since it has low self-attenuation effect at high energy. Since  $^{232}\text{Th}$  cannot be directly detected, the estimated activity *via* its progeny  $^{208}\text{Tl}$  and  $^{228}\text{Ac}$  using 2614.53 keV (35.63%), 583 keV (30.3%), and 911 keV, 338 keV, 463 keV. The gamma line of 1461 keV (10.7%) was used to resolve  $^{40}\text{K}$ . The activity concentrations were calculated according to the methods of Debertain and Helmer (2001) and Davisson and Evans (1952).

#### **2.4. Statistical evaluation for radionuclides measurement in the building materials samples**

Explanatory analysis of each radionuclide present in each building material was performed using descriptive statistics. Material classification and principal component analysis (PCA) were also executed to identify the contributions of each radionuclide to the building materials. Data evaluation was carried out using GraphPad Prism 6 for windows (GraphPad Software Inc.) and Unscrambler X (CAMO software AS, version 10.4).

### 3. Results and discussion

#### 3.1. Radioactivity concentrations

The detected naturally occurring radionuclides ( $^{226}\text{Ra}$ ,  $^{232}\text{Th}$ , and  $^{40}\text{K}$ ) from the building materials are presented in Table 2. The highest specific activities of  $^{226}\text{Ra}$ ,  $^{232}\text{Th}$ , and  $^{40}\text{K}$  in the samples are  $98.29 \pm 0.53 \text{ Bq kg}^{-1}$  (Goodwill Super Polish Porcelain tiles –  $600 \times 600 \text{ mm}$ ),  $174.14 \pm 7.76 \text{ Bq kg}^{-1}$  (Interlock Stone Site 2), and  $1829.40 \pm 15.10 \text{ Bq kg}^{-1}$  (BN Ceramics Floor tiles Nig –  $450 \times 450 \text{ mm}$ ), respectively, while the lowest values noted in the same samples were found to be  $17.64 \pm 0.59$  (Goodwill Ceramics – Nig –  $400 \times 250 \text{ mm}$ ),  $25.18 \pm 10.60 \text{ Bq kg}^{-1}$  (Elephant Portland Cement), and  $29.81 \pm 15.47 \text{ Bq kg}^{-1}$  (Golden Crown Ceramics (GCC) Nig –  $250 \times 400 \text{ mm}$ ), respectively. The mean value of  $^{226}\text{Ra}$  is  $45.72 \pm 0.55 \text{ Bq kg}^{-1}$ ; for  $^{232}\text{Th}$ , the mean value is  $65.90 \pm 8.89 \text{ Bq kg}^{-1}$ , whereas the mean value for  $^{40}\text{K}$  is  $487.32 \pm 15.20 \text{ Bq kg}^{-1}$ . These mean values obtained from this present study are distinctly higher than the corresponding values of worldwide average values of 35, 30, and  $400 \text{ Bq kg}^{-1}$  by factors of 1.31, 2.20, and 1.22, respectively (UNSCEAR 2000).

This higher mean value of  $^{40}\text{K}$  in the samples may be due to the ion-exchange of clay contents together with a simultaneous sedimentation of mineral particles containing uranium and thorium which could be attributed to the elevated activity concentrations found (Dragovic *et al.* 2015).

#### 3.2. Radiological health risk parameters

##### 3.2.1. Radium equivalent ( $Ra_{eq}$ ) activity

There is need to estimate the radium equivalent activity in the analyzed samples. To compare the activity concentrations of the present samples, which contain  $^{226}\text{Ra}$ ,  $^{232}\text{Th}$ , and  $^{40}\text{K}$ ,

**Table 2.** Activity concentrations in the measured building material samples.

Sample name/company of production	Sample ID	$^{226}\text{Ra}$ (Bq kg $^{-1}$ )	$^{232}\text{Th}$ (Bq kg $^{-1}$ )	$^{40}\text{K}$ (Bq kg $^{-1}$ )
Black Galaxy India (600× 300 mm)	BGI	81.51 ± 0.53	102.11 ± 7.87	871.72 ± 15.01
Blue Pearl India (600× 300 mm)	BPI	60.45 ± 0.53	79.86 ± 8.02	824.78 ± 15.01
BN Ceramics Floor tiles Nig (450× 450 mm)	BNC	58.18 ± 0.55	54.73 ± 9.63	1829.40 ± 15.10
BN Floor tiles Benia – (600× 600 cm)	BNF	44.28 ± 0.54	47.69 ± 9.11	635.28 ± 15.03
Dangote Cement (42.5N) Grade	DC	39.63 ± 0.54	25.90 ± 11.04	142.46 ± 15.28
Elephant Portland Cement	EPC	31.05 ± 0.55	25.18 ± 10.60	137.25 ± 15.37
Golden Crown Floor Ogum – (300× 300 mm)	GCF	41.77 ± 0.55	77.11 ± 8.40	126.33 ± 15.24
Golden Crown Ceramics Nig – (250× 400 mm)	GCC	19.82 ± 0.60	47.66 ± 8.80	29.81 ± 15.47
Gomez Spain (450 mm)	Gomez	29.70 ± 0.63	57.00 ± 8.76	701.85 ± 15.05
Goodwill Ceramics-Nig (400× 250 mm)	GWC	17.64 ± 0.59	41.27 ± 9.18	34.36 ± 15.40
Goodwill verified tile (400× 4000 mm)	GVT	80.93 ± 0.53	88.16 ± 8.36	460.87 ± 15.17
Green Pearl India (600× 300 mm)	GPI	41.99 ± 0.60	42.09 ± 9.24	181.40 ± 15.29
Goodwill Super Polish Porcelain tiles (600× 600 mm)	GSPP	98.29 ± 0.53	92.17 ± 8.28	551.93 ± 15.08
Iddris Floor tile – China (600× 600 mm)	IFT	69.87 ± 0.54	90.56 ± 8.89	323.10 ± 15.29
Interlock stone tiles Site 3-CU	IST	26.10 ± 0.58	86.55 ± 8.32	906.25 ± 15.27
Interlock Stone Site 1	IS1	27.38 ± 0.57	38.27 ± 9.82	510.16 ± 15.04
Interlock Stone Site 2	IS2	37.87 ± 0.57	174.14 ± 7.76	690.82 ± 15.14
IRIS Ceramics tiles Italy	IRIS	62.28 ± 0.53	37.61 ± 10.17	417.95 ± 15.13
Golden Crom Floor tiles Ogum – (300× 300 mm)	GCFO	41.77 ± 0.51	71.11 ± 7.44	126.33 ± 15.21
Golden Crown Ceramics Nig – (400× 400 mm)	GC	19.82 ± 0.50	47.66 ± 8.21	29.81 ± 15.34
Gomez (Spain) 450 mm	GS	29.70 ± 0.53	57.00 ± 8.71	701.85 ± 15.29
Mean values		45.72 ± 0.55	65.90 ± 8.89	487.32 ± 15.20

the radium equivalent concentration was used as the common index to ascertain the sum of the activities.  $Ra_{eq}$  activities were determined based on the estimation of  $370 \text{ Bq kg}^{-1}$  ( $10 \text{ pCi}^{-1}$ ) of  $^{226}\text{Ra}$ ,  $259 \text{ Bq kg}^{-1}$  ( $7 \text{ pCi}^{-1}$ ) of  $^{232}\text{Th}$ , and  $4810 \text{ Bq kg}^{-1}$  ( $130 \text{ pCi}^{-1}$ ) of  $^{40}\text{K}$ , each producing the same gamma ray dose rate (IAEA 1989, Krieger 1981, Beretka and Mathew 1985, Beck 1980).  $Ra_{eq}$  with unit as  $\text{Bq kg}^{-1}$  was calculated using Eq. (4.1).

$$Ra_{eq} = C_{Ra} + 1.43 C_{Th} + 0.077 C_K \quad (4.1)$$

where  $C_{Ra}$ ,  $C_{Th}$ , and  $C_K$  are the specific activities of  $^{226}\text{Ra}$ ,  $^{232}\text{Th}$ , and  $^{40}\text{K}$  measured in  $\text{Bq kg}^{-1}$ , respectively. The same external and internal gamma dose rate is produced from the radium equivalent activity. The maximum value of  $Ra_{eq}$  in building materials must be less than  $370 \text{ Bq kg}^{-1}$  as recommended by UNSCEAR (1988a). This amount is equivalent to  $1.5 \text{ n Gy}^{-1}$  (Krisiuk *et al.* 1971; Krieger 1981). The  $Ra_{eq}$  values obtained from this present study varied from 53.19 to  $340.083 \text{ Bq kg}^{-1}$  with the highest value of  $340.083 \text{ Bq kg}^{-1}$  noted in interlock stone Site 2, whereas the lowest value of  $53.19 \text{ Bq kg}^{-1}$  was noted in Elephant Portland Cement. The mean value for the analyzed samples was found to be  $172.71 \text{ Bq kg}^{-1}$ . From the measured samples, none of the  $Ra_{eq}$  values exceeded the recommended limit of  $370 \text{ Bq kg}^{-1}$  according to UNSCEAR (1988b); hence, this value for  $Ra_{eq}$  obtained in this study does not pose any radiological risk if used for construction buildings.

### 3.2.2. External hazard index ( $H_{ex}$ )

The external hazard index obtained from  $^{226}\text{Ra}$ ,  $^{232}\text{Th}$ , and  $^{40}\text{K}$  for this present study is shown in Table 3. The intent of applying this health hazard index, which is useful for the characterization of materials used for building, is to set limiting value on the acceptable equivalent dose recommended in a report by ICRP (1999). To limit the radiation dose from a construction material to  $1.5 \text{ mSv y}^{-1}$ , the value of  $H_{ex}$  must be less than unity (Erees *et al.* 2006, Ghose *et al.* 2012, Kobeissi *et al.* 2013, Gupta and Chauhan 2012). The external hazard index is also an additional criterion to assess the radiological suitability of building materials (UNSCEAR 2000, Avwiri *et al.* 2011) using Eq. (4.2).

$$H_{ex} = \frac{A_{Ra}}{370} + \frac{A_{Th}}{259} + \frac{A_K}{4810} \leq 1 \quad (4.2)$$

where  $A_{Ra} \sim A_U$ ,  $A_{Th}$ , and  $A_K$  are the average activity concentrations of  $^{226}\text{Ra}$ ,  $^{232}\text{Th}$ , and  $^{40}\text{K}$  in  $\text{Bq kg}^{-1}$ , respectively.

For the radiation hazard to be acceptable, it is recommended that  $H_{ex}$  must be less than unity. The estimated  $H_{ex}$  for all the samples varied from 0.210 to 0.918 with highest value noted in interlock from Site 2, whereas the lowest value of 0.237 reported in Dangote Cement (42.5N) Grade. The mean value of the estimated  $H_{ex}$  is 0.479 and was found to be lower than the recommended limit of 1. More so, this highest value from the interlock from Site 2 for this present study is still lower than the recommended value of  $\leq 1$  according to UNSCEAR (2000).

**Table 3.** The radium equivalent activity ( $\text{Bq kg}^{-1}$ ), internal and external hazard indices.

Sample name/company of production	Radium activity convention ( $R_{\text{eq}}$ ) ( $\text{Bq Kg}^{-1}$ )	External hazard index ( $H_{\text{ex}}$ )	Internal hazard index ( $H_{\text{in}}$ )
Black Galaxy India (600× 300 mm)	294.65	0.79	1.02
Blue Pearl India (600× 300 mm)	238.16	0.64	0.81
BN Ceramics Floor tiles Nig (450× 450 mm)	277.31	0.75	0.91
BN Floor tiles Benia – (600× 600 cm)	161.39	0.44	0.56
Dangote Cement (42.5N) Grade	87.64	0.24	0.34
Elephant Portland Cement	77.63	0.21	0.29
Golden Crom Floor tiles Ogum – (300× 300 mm)	161.76	0.44	0.55
Golden Crown Ceramics Nig – (250× 400 mm)	90.27	0.24	0.30
Gomez Spain (450 mm)	165.25	0.45	0.53
Goodwill ceramics – Nig (400× 250 mm)	79.30	0.21	0.26
Goodwill verified tile (400× 4000 mm)	242.46	0.65	0.87
Green Pearl India (600× 300 mm)	116.15	0.31	0.43
Goodwill Super Polish Porcelain tiles (600× 600 mm)	272.59	0.75	1.00
Iddris Floor tile – China (600× 600 mm)	224.23	0.61	0.79
Interlock stone tiles Site 3-CU	219.65	0.59	0.66
Interlock Stone Site 1	121.39	0.33	0.40
Interlock Stone Site 2	340.08	0.92	1.02
IRIS Ceramics tiles Italy	148.24	0.40	0.57
Golden Crom Floor tiles Ogum – (300× 300 mm)	53.18	0.41	0.53
Golden Crown Ceramics Nig – (250× 400 mm)	90.27	0.24	0.30
Gomez (Spain) 450 mm	165.25	0.45	0.53
Mean	172.71	0.48	0.60

### 3.2.3. Internal hazard index ( $H_{\text{in}}$ )

The internal hazard index obtained from this work is shown in Table 3. The internal exposure to radon and its progeny can be quantified using the internal index which is determined using Eq. (4.3) (Xinwei 2005; Alharbi *et al.* 2011; Beretka and Mathew 1985).

$$H_{\text{in}} = \frac{A_{\text{Ra}}}{185} + \frac{A_{\text{Th}}}{259} + \frac{A_{\text{K}}}{4810} \leq 1 \quad (4.3)$$

For the utilization of a building material to be considered safe, the internal hazard must be less than 1 (Ghose *et al.* 2012; Alharbi *et al.* 2011). In the present study, the  $H_{\text{in}}$  ranged from 0.26 to 1.02 with the highest value of 1.02 noted in Interlock Stone Site 2 sample whereas the lowest value of 0.262 reported in Goodwill Ceramics – Nig (400 × 250 mm) tile sample. The mean value of all the samples is 0.603 which is less than the world average of <1, indicating that the internal hazard is lower than the critical value. The internal hazard indices of Black Galaxy India (600 × 300 mm) marble sample, Interlock Stone Site 2 and Goodwill Super Polish Porcelain tiles (600 × 600 mm) are 1.02, 1.02 and 1 respectively. These values are higher than the recommended safe level when compared with safe value by UNSCEAR (2000), Ghose *et al.* (2012), Alharbi *et al.* (2011) and are considered not safe for building purposes.

### 3.2.4. Absorbed gamma dose rate ( $D_{\text{R}}$ )

The absorbed dose rate indoor air ( $D_{\text{R}}$ ) and the corresponding annual effective doses (AEDR) contributed to gamma ray emission from the natural radionuclide ( $^{226}\text{Ra}$ ,  $^{232}\text{Th}$ , and  $^{40}\text{K}$ ) in building materials which were estimated according to formulas initiated by



UNSCEAR (2000) and EC (1999). In the UNSCEAR and European Commission reports, the dose conversion coefficients were calculated for the center of a standard room. The  $D_R$  was estimated using Eq. (4.4) as given by EC (1999) and UNSCEAR (2000).

$$D_R = 0.436 A_{Ra} + 0.599 A_{Th} + 0.0417 A_K \text{ (nGy h}^{-1}\text{)} \quad (4.4)$$

Considering the absorbed dose rates presented in Table 4, the absorbed dose rate varied from 34.51 to 151.49 nGy h<sup>-1</sup> with the highest value of 151.49 reported in interlock material from Site 2 whereas the lowest value of 34.51 nGy h<sup>-1</sup> was noted in Elephant Portland Cement as shown in Table 4. Comparing the highest absorbed dose rate in this present study with the standard limit safe level of 84 nGy h<sup>-1</sup> recommended by UNSCEAR (1988a), is higher by a factor of 1.9. The mean value of the analyzed samples is found to be 81 nGy h<sup>-1</sup> which is lower than the world average of 84 nGy h<sup>-1</sup>. The average absorbed dose due to the existence of <sup>226</sup>Ra, <sup>232</sup>Th, and <sup>40</sup>K in the samples is 81 nGy h<sup>-1</sup>. This value is higher than the world's average value of 59 nGy h<sup>-1</sup> (UNSCEAR 2000; Xinwei 2005) by a factor of 1.04.

### 3.2.5. The external absorbed dose rate ( $D_{out}$ )

Details of the estimated outdoor external absorbed doses due to the existence of <sup>226</sup>Ra, <sup>232</sup>Th, and <sup>40</sup>K are presented in Table 4. The external absorbed dose rate ( $D_{out}$ ) in nGy h<sup>-1</sup> delivered by the radionuclides under investigation to the general public in the outdoor air was calculated using equation 2, which has been presented by researchers (Rahman *et al.* 2013; Khandaker *et al.* 2012; Ahmed 2005)

**Table 4.** The absorbed gamma dose rate, internal and external absorbed dose rate.

Company of production	Dose rate ( $D_R$ )	External absorbed dose rate ( $D_{out}$ )	Internal absorbed dose rate ( $D_{in}$ )
Black Galaxy India (600 × 300 mm)	135.68	140.06	196.08
Blue Pearl India (600 × 300 mm)	110.56	114.31	160.03
BN Ceramics Floor tiles Nig (450 × 450 mm)	136.22	140.10	196.15
BN Floor tiles Benia – (600 × 600 cm)	75.75	77.92	109.09
Dangote Cement (42.5N) Grade	39.89	40.22	56.31
Elephant Portland Cement	35.28	35.86	50.20
Golden Crom Floor tiles Ogum – (300 × 300 mm)	71.14	74.34	104.07
Golden Crown Ceramics Nig – (250 × 400 mm)	39.19	41.30	57.82
Gomez Spain (450 mm)	77.42	80.74	113.03
Goodwill Ceramics – Nig (400 × 250 mm)	34.51	36.34	50.87
Goodwill verified tile (400 × 4000 mm)	109.86	112.83	157.96
Green Pearl India (600 × 300 mm)	52.39	53.63	75.08
Goodwill Super Polish Porcelain tiles (600 × 600 mm)	124.10	126.83	177.56
Iddris Floor tile – China (600 × 600 mm)	100.45	103.74	145.24
Interlock stone tiles Site 3-CU	102.13	107.59	150.63
Interlock Stone Site 1	57.04	59.06	82.69
Interlock Stone Site 2	151.48	161.29	225.81
IRIS Ceramics tiles Italy	68.92	69.55	97.37
Golden Crom Floor tiles Ogum – (300 × 300 mm)	67.52	70.37	98.52
Golden Crown Ceramics Nig – (250 × 400 mm)	39.19	41.30	57.82
Gomez (Spain) 450 mm	77.42	80.74	113.03
Mean	81.24	84.20	117.87

The  $D_{out}$  was estimated using Eq. (4.5) as given by EC (1999).

$$D_{out} = 0.427 C_{Ra} + 0.662 C_{Th} + 0.0432 C_K \text{ (nGy h}^{-1}\text{)} \quad (4.5)$$

where  $C_{Ra}$ ,  $C_{Th}$ , and  $C_K$  are the specific activities of  $^{226}\text{Ra}$ ,  $^{232}\text{Th}$ , and  $^{40}\text{K}$  measured in  $\text{Bq kg}^{-1}$ , respectively. The  $D_{out}$  in Table 4 ranged from 35.86 to 161.30  $\text{nGy h}^{-1}$  with the mean value of 84.20  $\text{nGy h}^{-1}$ . This highest value of 161.30  $\text{nGy h}^{-1}$  was reported in interlock Site 2 sample, whereas the lowest value of 35.86  $\text{nGy h}^{-1}$  was reported in Elephant Portland Cement. This mean value of 84.20  $\text{nGy h}^{-1}$  may not contribute to gamma activity of 370  $\text{Bq kg}^{-1}$  that will keep higher external dose rate up to 1.5  $\text{mSv y}^{-1}$  according to UNSCEAR (2000).

### 3.2.6. The internal absorbed dose rate ( $D_{in}$ )

Considering the fact that the indoor dose contribution is 1.4 times higher than the outdoor dose contribution, the gamma dose indoor ( $D_{in}$ ) in the indoor environment is delivered by radionuclides (gamma emission from  $^{226}\text{Ra}$ ,  $^{232}\text{Th}$ , and  $^{40}\text{K}$ ) in the assessed construction materials using Eq. 4.6 by UNSCEAR (2000), Usikalu *et al.* (2011), Arabi *et al.* (2008), and Debertain and Helmer (2014).

$$D_{in} = 1.4 D_{out} \quad (4.6)$$

The internal absorbed dose listed in Table 4 for this present study varied from 50.20 to 1191.93  $\text{nGy h}^{-1}$  with a mean value of 225.81  $\text{nGy h}^{-1}$  with the highest value noted in Interlock Stone Site 2 whereas the lowest value was reported in Elephant Portland Cement as shown in Table 4.

### 3.2.7. Annual effective dose rate (AEDR)

The indoors annual effective dose equivalent received by human is estimated from the indoor internal dose rate ( $D_{in}$ ), occupancy factor which is defined as the level of human occupancy in an area in proximity with radiation source, which is given as 80% of 8760 h in a year, and the conversion factor of 0.7  $\text{SvG y}^{-1}$  which is used to convert the absorbed dose in air to effective dose received by the adult (ICRP 1991). The annual dose received by the building occupants due to the activity emanating from the building materials was determined using Eq. 4.7 (Usikalu *et al.* 2017).

$$H_R \text{ (mSv)} = D_R \text{ (nGy h}^{-1}\text{)} \times 8766 \text{ h} \times 0.8 \text{ (occupancy factor)} \\ \times 0.7 \text{ SvG y}^{-1} \text{ (conversion factor)} \times 10^{-6} \quad (4.7)$$

The value of the AEDR from the analyzed samples ranged from 0.262634 to 0.744  $\text{mSv y}^{-1}$  with a mean value of 0.43  $\text{mSv y}^{-1}$  as presented in Table 5. The sample with highest AEDR is interlock stone Site 2 and Black Galaxy India (600 × 300 mm) as shown in Table 5, with a value of 0.666 and 0.744  $\text{mSv y}^{-1}$ , respectively, whereas Golden Crown Ceramics Nig (250 × 400 mm) reported the lowest AEDR. The mean values of 0.399  $\text{mSv y}^{-1}$  annual effective dose from the samples surpass the world's average value of 0.07  $\text{mSv y}^{-1}$  according to UNSCEAR (2000) by a factor 5.7.

**Table 5.** The annual effective dose, gamma activity index, and alpha index.

Sample name/company of production	Annual effective dose (AEDR (mSv y <sup>-1</sup> ))	Gamma activity index (I <sub>γ</sub> )	Alpha index (I <sub>α</sub> )
Black Galaxy India (600× 300 mm)	0.67	1.07	0.41
Blue Pearl India (600× 300 mm)	0.54	0.88	0.30
BN Ceramics Floor tiles Nig (450× 450 mm)	0.67	1.08	0.29
BN Floor tiles Benia – (600× 600 cm)	0.37	0.60	0.22
Dangote Cement (42.5N) Grade	0.20	0.31	0.20
Elephant Portland Cement	0.17	0.28	0.16
Golden Crom Floor tiles Ogum – (300× 300 mm)	0.35	0.57	0.21
Golden Crown Ceramics Nig – (250× 400 mm)	0.19	0.31	0.20
Gomez Spain (450 mm)	0.38	0.62	0.15
Goodwill ceramics – Nig (400× 250 mm)	0.17	0.28	0.09
Goodwill verified tile (400× 4000 mm)	0.54	0.86	0.40
Green Pearl India (600× 300 mm)	0.26	0.41	0.21
Goodwill Super Polish Porcelain tiles (600× 600 mm)	0.61	0.97	0.49
Iddris Floor tile – China (600× 600 mm)	0.49	0.793	0.35
Interlock stone tiles Site 3-CU	0.50	0.82	0.13
Interlock Stone Site 1	0.28	0.45	0.14
Interlock Stone Site 2	0.74	1.23	0.89
IRIS Ceramics tiles Italy	0.34	0.53	0.31
Golden Crom Floor tiles Ogum – (300× 300 mm)	0.33	0.54	0.21
Golden Crown Ceramics Nig – (250× 400 mm)	0.19	0.31	0.09
Gomez (Spain) 450mm	0.38	0.62	0.15
Mean	0.40	0.64	0.27

### 3.2.8. Gamma activity index representations

The distribution of values of gamma index for the building materials measured in this present study is presented in Table 5. The gamma index is correlated with the annual dose rate attributed to excess external gamma radiation caused by superficial materials. The value of  $I_{\gamma r} \leq 2$  correspond to a dose rate of criterion of  $0.30 \text{ mSv y}^{-1}$ , whereas  $2 < I_{\gamma} \leq 6$  corresponds to a criterion of  $1 \text{ mSv y}^{-1}$ , whereas a gamma activity index  $\leq 0.5$  corresponds to  $0.3 \text{ mSv y}^{-1}$  if the materials are used in bulk quantity (EC 1990; Anjos *et al.* 2010). If the  $I_{\gamma}$  for building material is greater than 6, such material should be avoided since it corresponds to dose rate higher than  $1 \text{ mSv y}^{-1}$  (EC 1999; Kant *et al.* 2006) which is presumed to be the highest dose rate value recommended for the general public (UNSCEAR 2000).

The gamma index representation ( $I_{\gamma r}$ ) is estimated using Eq. (4.8) as presented by OECD (1979).

$$I_{\gamma} = \frac{\text{CRa}}{300 \text{ Bq kg}^{-1}} + \frac{\text{CTh}}{200 \text{ Bq kg}^{-1}} + \frac{\text{CK}}{3000 \text{ Bq kg}^{-1}} \quad (4.8)$$

The gamma index for the measured building materials varied from 0.275 to 1.23 with the highest value noted in interlock stone Site 2, whereas the lowest value of 0.275 reported in Elephant Portland Cement with a mean value of 0.644. It can be observed that all samples are lower than 4, the average value. Since these materials are used for building, it is appropriate to consider the level of impact of the average value of these different materials. With this average value of 0.644, it indicates a dose rate of lower than  $0.30 \text{ mSv y}^{-1}$ . As such, the annual effective dose delivered by the building materials is smaller than the annual effective dose constraints of  $1 \text{ mSv y}^{-1}$ . It could be suggested that these building materials can be exempted from restrictions concerning radiological and radioactivity risks.

### 3.2.9. Alpha index

The alpha index has been developed as an assessment of the excess alpha radiation exposure caused by the inhalation originating from building materials. The alpha index in this present study was calculated using Eq. 4.9 (Righi and Bruzzi 2006; Xinwei 2005):

$$I_{\alpha} = \frac{C_{Ra}}{200 \text{ Bq kg}^{-1}} \quad (4.9)$$

where  $C_{Ra}$  is the activity concentration of radium ( $\text{Bq kg}^{-1}$ ) in building materials. If the radium activity level in building material exceeds the values of  $200 \text{ Bq kg}^{-1}$ , there is possibility that the radon exhalation from the material could cause indoor radon concentrations exceeding  $200 \text{ Bq m}^{-3}$ . The International Commission on Radiation Protection recommended an action level of  $200 \text{ Bq m}^{-3}$  for radon in dwellings (ICRP 1994; EC 1999). At the same time, if this radium activity level is below  $100 \text{ Bq kg}^{-1}$ , it shows that radon exhalation from building materials may not likely cause indoor concentration greater than  $200 \text{ Bq m}^{-3}$  (Xinwei and Xiaolon (2008)). It is reported that the recommended exempted value and the recommended upper limit for radon concentrations are  $100 \text{ Bq kg}^{-1}$  and  $200 \text{ Bq kg}^{-1}$ , respectively, in building materials (RPA 2000). It is noted that the upper limit of radon concentration ( $I_{\alpha}$ ) is equal to 1 (Tufail *et al.* 2007). The results of this present study show that the radon concentration varied from 0.1275 to 0.4075, respectively, in Table 5. With this lower value, it indicated that the radon exhalation from all the analyzed samples would cause indoor concentration lower than  $200 \text{ Bq kg}^{-1}$ .

### 3.2.10. Activity utilization index (AUI)

Estimation of the activity utilization index from different combinations of the  $^{226}\text{Ra}$ ,  $^{232}\text{Th}$ , and  $^{40}\text{K}$  in building materials can be obtained using the following Eq. 4.8 (UNSCEAR, 1993):

$$\text{AUI} = \left( \frac{C_{Ra}}{50 \text{ Bq kg}^{-1}} \right) f_{Ra} + \left( \frac{C_{Th}}{50 \text{ Bq kg}^{-1}} \right) f_{Th} + \left( \frac{C_K}{500 \text{ Bq kg}^{-1}} \right) f_K \quad (4.8)$$

where  $C_{Th}$ ,  $C_{Ra}$ , and  $C_K$  are the actual values of the activities per unit mass ( $\text{Bq kg}^{-1}$ ) of  $^{232}\text{Th}$ ,  $^{226}\text{Ra}$ , and  $^{40}\text{K}$ , respectively, in the assessed building materials.  $f_{Th}$ ,  $f_{Ra}$ , and  $f_K$  are the fractional contributions of the total dose rate in air attributed to gamma radiation from the actual activity concentration from the measured radionuclides. The activity utilization index is 2 by definition and is deemed to imply a dose rate of  $80 \text{ nGy h}^{-1}$  (UNSCEAR 1993). In this present study, the AUI varied from 1.40 to 5.62 with the highest value of 5.62 noted in interlock stone Site 2 while the lowest value of 1.40 was noted in Elephant Portland Cement sample as shown in Table 6. The values are presented in Table 4.5. It can be observed that these values satisfied the  $\text{AUI} < 2$ , which corresponds to the annual effective dose of  $< 0.3 \text{ mSv y}^{-1}$  according to El-Gamal *et al.* (2007) and Sahu *et al.* (2014) except Black Galaxy India ( $600 \times 300 \text{ mm}$ ), Blue Pearl India ( $600 \times 300 \text{ mm}$ ), Goodwill verified tile ( $400 \times 4000 \text{ mm}$ ), Gomez Spain ( $450 \text{ mm}$ ), Goodwill Super Polish Porcelain tiles ( $600 \times 600 \text{ mm}$ ), and Iddris Floor tile – China ( $600 \times 600 \text{ mm}$ ). Interlock Stone Site 2 and Gomez Spain ( $450 \text{ mm}$ ) should be monitored if used for construction of building as well as their exposure to dwellers.

**Table 6.** The activity utilization index and excess lifetime cancer risk.

Sample name/company of production	Activity utilization index (AU)	Excess lifetime cancer risk (ELCR $\times 10^{-3}$ )
Black Galaxy India (600 $\times$ 300 mm)	5.41	0.0023
Blue Pearl India (600 $\times$ 300 mm)	4.46	0.0019
BN Ceramics Floor tiles Nig (450 $\times$ 450 mm)	5.92	0.0023
BN Floor tiles Benia – (600 $\times$ 600 cm)	3.11	0.0013
Dangote Cement (42.5N) Grade	1.60	0.0007
Elephant Portland Cement	1.40	0.0006
Golden Crom Floor tiles Ogum – (300 $\times$ 300 mm)	2.63	0.0012
Golden Crown Ceramics Nig – (250 $\times$ 400 mm)	1.41	0.0007
Gomez Spain (450 mm)	3.14	0.0013
Goodwill ceramics – Nig (400 $\times$ 250 mm)	1.25	0.0006
Goodwill verified tile (400 $\times$ 4000 mm)	4.30	0.0019
Green Pearl India (600 $\times$ 300 mm)	2.04	0.0009
Goodwill Super Polish Porcelain tiles (600 $\times$ 600 mm)	4.91	0.0021
Iddris Floor tile – China (600 $\times$ 600 mm)	3.85	0.0017
Interlock stone tiles Site 3-CU	4.07	0.0018
Interlock Stone Site 1	2.33	0.0010
Interlock Stone Site 2	5.62	0.0026
IRIS Ceramics tiles Italy	2.83	0.0012
Golden Crom Floor tiles Ogum – (300 $\times$ 300 mm)	2.51	0.0012
Golden Crown Ceramics Nig – (250 $\times$ 400 mm)	1.41	0.0007
Gomez (Spain) 450 mm	3.14	0.0013
Mean	3.21	0.0014

### 3.2.11. Excess lifetime cancer risk (ELCR)

One of the radiological parameters calculated in this study was the excess lifetime cancer risk (ELCR) which was calculated using Equation 8 by Taskin *et al.* (2009) and Beck (1980). The ELCR is presented in Table 4.5.

$$\text{ELCR} = \text{AEDR} \times \text{DL} \times \text{RF} \quad (4.9)$$

where AEDR, DL, and RF are the annual effective dose equivalent, Duration of life (70 y), and risk factor ( $0.05 \text{ Sv}^{-1}$ ), respectively. The risk factor is the fatal cancer risk per Sievert. For stochastic effect, the International Commission on the Radiological Protection (ICRP 60) uses a value of 0.05 for the general public (Taskin *et al.* 2009; Holm and Ballestra 1989). The values estimated from this study ranges from 0.0007 to 0.0023 with highest value of 0.0023 found in Black Galaxy India and BN Ceramic Tiles, whereas the lowest value of 0.0007 was noted in Dangote as presented in Table 6. The mean value of ELCR from the present study was 0.0014 which is higher than the world average value of  $0.29 \times 10^{-3}$  according to UNSCEAR (2000) by a factor of 4.8.

### 3.3. Statistical analysis Using Principal Component Analysis (PCA)

PCA is a technique adopted by several researchers to explain the differences that exist in large data in which their variables are connected. It reduces the complexity of interpreting large data set by means of dimensionality approach (Emenike *et al.* 2017). In this study, the PCA was conducted and from the screen plot, two components were produced (PC1 and PC2). Both components amount up to 99% of the total variance as shown in the scree plot (Figure 2). PC1 contributed 98.48% while PC2 added less than

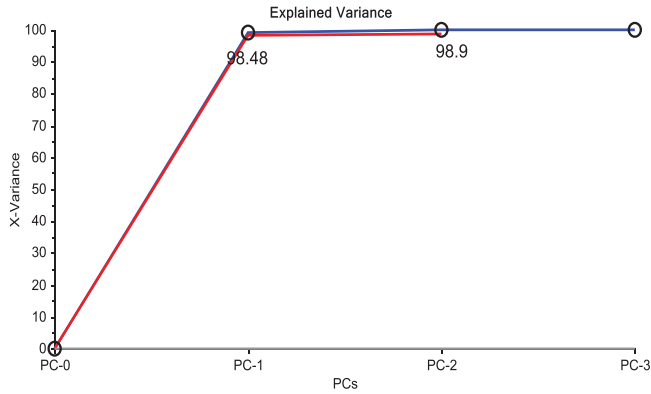


**Figure 2.** Scree plot of explained variance for individual principal components.

1% (0.42%) to the entire variance. The important radionuclide parameter controlling the process is often located in PC1. This may be due to the presence of filler such as quartz ( $\text{SiO}_2$ ), alumina ( $\text{Al}_2\text{O}_3$ ), or zirconia ( $\text{ZrO}_2$ ) which gives mechanical strength to the tile. Within the explained variance of PC1 (Figure 3), strong positive loadings were recorded in  $^{40}\text{K}$  ( $r = 1.000$ ). There also exist a strong positive loading produced by  $^{232}\text{Th}$  ( $r = 0.9398$ ) and a moderate positive loading by  $^{226}\text{Ra}$  in PC2 which may be due to the constituent of geologic materials such as kaoline, plasticity clay, feldspar, granite, as well as magnesia bodies such as calcium and additives (plasticizers, binders). Building materials with similar characteristics and information within the samples can be identified using the score plot (Figure 4). From the results, GCC, GPI, GWC, EPC, and DC possess similar attributes. These samples are characterized with loadings on PC1 having values  $-458.1885$ ,  $-306.4048$ ,  $-453.8252$ ,  $-351.1153$ , and  $-345.7419$ , respectively. Other materials having similar composition include GCF and GCFO (loadings of  $-360.7882$  and  $-360.6501$ , respectively); Gomez and BNF (loadings of  $213.9588$  and  $147.4553$ , respectively); GSPP, GVT, and IFT (loadings of  $66.1005$ ,  $-25.3152$ , and

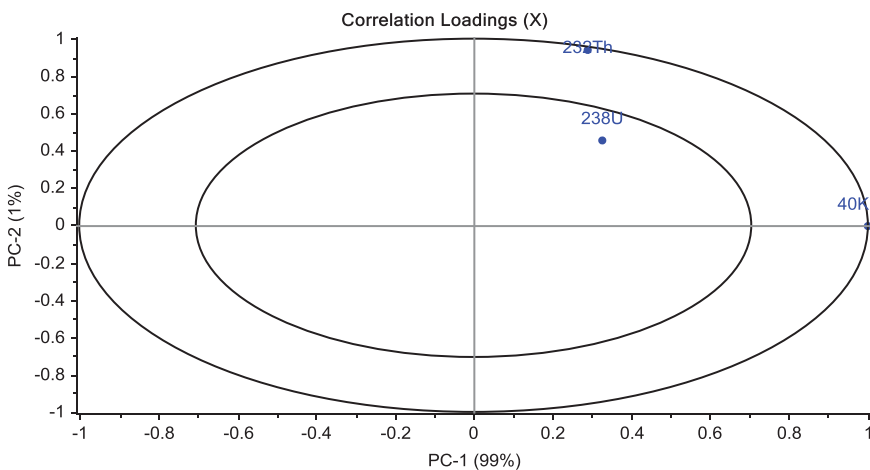


**Figure 3.** Correlation loadings with respect to components.

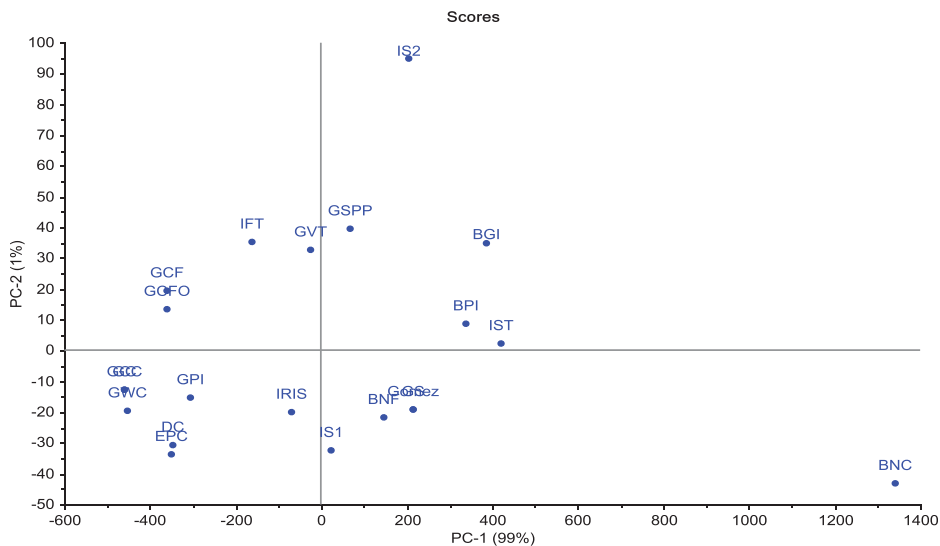


**Figure 4.** Scree plot of individual samples with respect to principal components.

−163.1648, respectively); BPI and IST (loadings of 337.8973 and 418.8911, respectively). The leverage plot (Figure 5) shows the contribution of individual materials on the respective components. In PC1, the highest contributors are BNC, GCC, GC, and GWC. PC2 had contributors emanating from BNC, IS2, BGI, and EPC. This study considered the correlation range of 0.1–0.29 as a weak relationship, 0.3–0.69 as moderate relationship and 0.7–0.99 as strong relationship. Within the correlation, there exist a moderate relationship between  $^{226}\text{Ra}$  and  $^{232}\text{Th}$  ( $r = 0.3737$ ), and moderate relationship between  $^{40}\text{K}$  and  $^{226}\text{Ra}$  ( $r = 0.3265$ ). The results obtained corroborate the significant

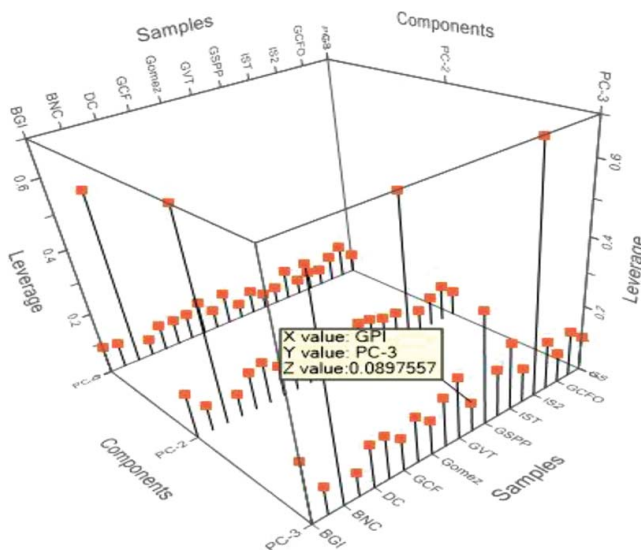


**Figure 5.** Leverage plot showing the respective contributions of samples to the principal components.

ratio existing between  $^{226}\text{Ra}$  and  $^{232}\text{Th}$ . similar correlation was obtained in previous works by Omeje *et al.* 2014.

#### 4. Conclusion

In this study, the activity concentrations of  $^{226}\text{Ra}$ ,  $^{232}\text{Th}$ , and  $^{40}\text{K}$  in commercial building materials were measured to estimate the radiological health risk parameters for the evaluation of the potential lifetime cancer risk to human health. Statistically, there was a slightly higher relationship between  $^{226}\text{Ra}$  and  $^{232}\text{Th}$ . A slightly lower relationship was found between the  $^{40}\text{K}$  and  $^{226}\text{Ra}$ . The mean value of the absorbed dose rate of the analyzed samples was found to be  $81 \text{ nGy h}^{-1}$ , which is lower than the world average of  $84 \text{ nGy h}^{-1}$  by a factor of 1.9. The mean value of  $0.399 \text{ mSv y}^{-1}$  for annual effective dose from the samples surpassed the world's average value of  $0.07 \text{ mSv y}^{-1}$  by a factor 5.7. The value of some AUI satisfies the  $\text{AUI} < 2$ , which corresponded to the annual effective dose of  $< 0.3 \text{ mSv y}^{-1}$ . The estimated mean value of excess lifetime cancer risk (ELCR) was 0.0014, which is higher than the world average value of  $0.29 \times 10^{-3}$ . The result of the activity utilization index showed that Black Galaxy and BN Ceramic Tile should be monitored if used for construction of buildings due to excess lifetime cancer risk exposure to dwellers. This study would help in regulating and monitoring the radioactivity level effect from building materials.

#### Acknowledgment

We acknowledge Covenant University management for their encouragement and support to execute this research. We are also thankful to Department of Material Science and Engineering, Obafemi Awolowo, and Ile-Ife for providing full equipment for grinding, crushing, and sieving the building material samples used for this research.

#### Funding

The authors would like to thank the management of Covenant University through Covenant University Center for Research Innovation and Discovery (CUCRID) research grant scheme (No: CUCRID/VC/17/02/02/06-FS) for their 100% financial support of the present study.

#### ORCID

Omeje M.  <http://orcid.org/0000-0001-9124-1093>

Emenike C. PraiseGod  <http://orcid.org/0000-0001-6778-6413>

Usikalu M. R.  <http://orcid.org/0000-0003-2233-4055>

Akinwumi Sayo A.  <http://orcid.org/0000-0001-5373-1067>

#### References

Ahmed NK. 2005. Measurement of natural radioactivity in building materials in Qena city, Upper Egypt. *J Environ Radioact* 83:91–99



- Anjos RM, Umisedo N, da Silva AAR, *et al.* 2010. Occupational exposure to radon and natural gamma radiation in the La Carolina, a former gold mine in San Luis Province, Argentina. *J Environ Radioact* 101:153–158
- Akkurt I, Altindag R, Onargan T, *et al.* 2007. The properties of various igneous rocks for  $\gamma$ -ray shielding. *Constr Build Mater* 21:2078–82. <https://doi.org/10.1016/j.conbuildmat.2006.05.059>
- Alharbi WR, Al Zahrani JH, and Adel GE Abbady. 2011. Assessment of radiation hazard indices from granite rocks of the southeastern Arabian Shield, Kingdom of Saudi Arabia. *Aust J Basic Appl Sci* 5:672–82
- Alnour I, Wagiran H, Ibrahim N, *et al.* 2012. Natural radioactivity measurements in the granite rock of quarry sites, Johor, Malaysia. *Radiat Phys Chem* 81(12):1842–7. *Annexes*. United Nations. New York. <https://doi.org/10.1016/j.radphyschem.2012.08.005>
- Amin SA, and Naji M. 2013. Natural radioactivity in different commercial ceramic samples used in yemeni buildings. *J Radiat Phys Chem* 86:37–41
- Arabi AM, Ahmed NK, and Salahel DK. 2008. Assessment of terrestrial gamma radiation doses for some Egyptian granite samples. *Radiat Prot Dosim* 128(3):382–5. <https://doi.org/10.1093/rpd/ncm367>
- Avwiri GO, Nte FU, and Olanrewaju AI. 2011. Determination of radionuclide concentration of landfill at Eliozi, Port Harcourt, Rivers State. *Sci Africana* 10(1)
- Beck HL. 1980. Exposure rate conversion factors for radionuclides deposited on the ground. Department of Energy. Environmental Measurements Lab: New York, USA
- Beretka J, and Mathew, PJ. 1985. Natural radioactivity of Australian building materials, industrial waste sand by-products. *Health Phys* 48:87–95. <https://doi.org/10.1097/00004032-198501000-00007>
- Billman HG. 1992. Offshore stratigraphy and paleontology of Dahomey (Benin) Embayment. *NAPE Bull* 70(02):121–30
- Currie LA. 1968. Limits for qualitative detection and quantitative determination. Application to radiochemistry. *Anal Chem* 40(3):586–93. <https://doi.org/10.1021/ac60259a007>
- Davisson CM, and Evans RD. 1952. Gamma-ray absorption coefficients. *Rev Mod Phys* 24(2):79. <https://doi.org/10.1103/RevModPhys.24.79>
- Debertin K, and Helmer RG. 2001. Gamma- and x-ray spectrometry with semiconductor detectors. 1st ed. Oxford, Amsterdam, North-Holland
- Debertin K, and Helmer RG. 2014. Gamma- and X-Ray Spectrometry with Semiconductor Detectors. North-Holland, Amsterdam
- Dragović S, Petrović J, Dragović R, *et al.* 2015. The Influence of Edaphic Factors on Spatial and Vertical Distribution of Radionuclides in Soil. In: Walther C., Gupta D. (eds.) *Radionuclides in the Environment*, pp 61–80 Springer, Cham. doi [https://doi.org/10.1007/978-3-319-22171-7\\_3](https://doi.org/10.1007/978-3-319-22171-7_3)
- EC (European Commission). 1999. Radiological protection principles concerning the natural radioactivity of building materials. Radiation protection 112. Directorate General Environment, Nuclear Safety and Civil Protection (Geneva: EC)
- El-Gamal A, Nasr S, and El-Taher A. 2007. Study of the spatial distribution of natural radioactivity in the upper Egypt Nile River sediments. *Radiation measurements*, 42(3):457–465
- Emenike PC, Tenebe TI, Omeje M, *et al.* 2017. Health risk assessment of heavy metal variability in sachet water sold in Ado-Odo Ota, South-Western Nigeria. *Environ Monit Assess* 189: 1–16. <https://doi.org/10.1007/s10661-017-6180-3>
- Erees FS, Dayanıklı SA, and Çam S. 2006. Natural radionuclides in the building materials used in Manisa city, Turkey. *Indoor Built Environ* 15(5):495–8. <https://doi.org/10.1177/1420326X06069059>
- Ghose S, Kh Asaduzzaman, and Zaman N. 2012. Radiological significance of marble used for construction of dwellings in Bangladesh. *Radioprot* 47(1):105–18. <https://doi.org/10.1051/radiopro/2011158>
- Gupta M, and Chauhan RP. 2012. Estimation of low-level radiation dose from some building materials using gamma spectroscopy. *Indoor Built Environ* 21(3):465–73. <https://doi.org/10.1177/1420326X11414283>
- Gupta M, Gupta BP, Chauhan A, *et al.* 2009. Ocular morbidity prevalence among school children in Shimla, Himachal, North India. *Indian J Ophthalmol* 57(2):133–8

- Hamby DM, and Tynybekov AK. 2002. Uranium, Thorium, and Potassium in soils along the shore of the lake Issyk-Kyol in the Kyrgyz Republic. *Environ Monitor Assess* 73:01–108. <https://doi.org/10.1023/A:1013071414970>
- Holm E, and Ballestra S. 1989. *Measurement of Radionuclides in Food and the Environment, A Guidebook*. IAEA Tech. Rept. Vienna, Ser
- ICRP. 1990. Annual limits on intake of radionuclides by workers based on the recommendations. *Annals on the ICRP*, ICRP publication 67, Oxford Press. (ICRP, 1999)
- ICRP. 1991. *Publication 60: 1990 Recommendations of the International Commission on Radiological Protection*. Elsevier Health Sciences
- ICRP (Internal Commission on Radiological Protection). 1994. Protection against Rn-222 at home and at work. ICRP publication 65; *Ann. ICRP* 23(2):1–48
- ICRP. 1999. Protection of the public in situations of prolonged radiation exposure. *Publication 82, Ann. ICRP* 29(1–2), Elsevier Sciences, B.V. International Commission on Radiological Protection IAEA (International Atomic Energy Agency). 1989. Construction and use of calibration facilities for radiometric field equipment. *Technical Reports Series no.309*, IAEA, Vienna
- Jones HA, and Hockey RD. 1964. The geology of part of southwestern Nigerian. *Bull Geol Surv Niger* 31(4):101
- Juvanbot DI, Izam MM, Nyam GG, *et al.* 2014. Indoor and outdoor Gamma Dose rate Exposure Levels In Major Commercial Building materials Distribution Outlets in Jos, Plateau State Nigeria. *Asian Review of Environmental and Earth Sciences*. Vo1. no 1, 5–7 June 2014. Asian Outline Journal Publishing Group
- Kant K, Upadhyay SB, Sonkawade RG, *et al.* 2006. Radiological risk assessment of use of phosphate fertilizers in soil. *Iranian J Radiat Res* 4(2):63–70
- Khandaker MU, Jojo PJ, Kassim HA, *et al.* 2012. Radiometric analysis of construction materials using HPGe gamma-ray spectrometry. *Radiat Prot Dosim* 152:33–37
- Kobeissi MA, El-Samad O, Rachidi I. 2013. Health assessment of natural radioactivity and radon exhalation rate in granites used as building materials in Lebanon. *Radiat Prot Dosim* 153:342–51. <https://doi.org/10.1093/rpd/ncs110>
- Krieger R. 1981. Radioactivity of construction materials. *Betonwerk Fertigteil Techn* 47:468–473
- Krisiuk EM, Tarasov SI, Shamov VP, *et al.* 1971. A study on radioactivity in building materials. *Res Inst Radiat Hyg, Leningr* 144
- O'Brien RS. 1997. Gamma doses from phosphogypsum plaster-board. *Health Phys* 72:92–6. <https://doi.org/10.1097/00004032-199701000-00012>
- OECD (Organization for Economic Co-operation and Development). 1979. Exposure to radiation from natural radioactivity in building materials. Report by a group of experts of the OECD Nuclear Energy Agency
- Olabode SO. 2006. Siliciclastic slope deposits from the Cretaceous Abeokuta Group, Dahomey (Benin) Basin, southwestern Nigeria. *J Afr Earth Sci* 46:187–200. <https://doi.org/10.1016/j.jafrearsci.2006.04.008>
- Omatsola ME, and Adegoke OS. 1981. Tectonic evolution and Cretaceous stratigraphy of the Dahomey basin. *Nigeria Geol* 18(51):130–7
- Omeje M, Wagiran H, Ibrahim N, *et al.* 2013. Comparison of  $^{238}\text{U}$ ,  $^{232}\text{Th}$ , and  $^{40}\text{K}$  in different layers of subsurface structures in Dei-Dei and Kubwa, Abuja
- Omeje M, Wagiran H, Ibrahim N, *et al.* 2014. Natural radioactivity and geological influence on subsurface layers at Kubwa and Gosa area of Abuja, Northcentral Nigeria. *J Radioanal Nucl Chem* 303:821–30
- Omeje M, Olusegun O. A, Emmanuel S. J, *et al.* 2017. Proceedings of International Conference on Science and Sustainable Development (ICSSD) “The Role of Science in Novel Research and Advances in Technology” Center for Research, Innovation and Discovery, Covenant University, Nigeria *J Inform and Math Sci* 9(2):423–36
- Qureshi AA, Tariq S, Din KU, *et al.* 2014. Evaluation of excessive lifetime cancer risk due to natural radioactivity in the rivers sediments of Northern Pakistan. *J Radiat Res Appl Sci* 7(4):438–47. <https://doi.org/10.1016/j.jrras.2014.07.008>

- Rahman SU, Rafique M, and Jabbar AM. 2013. Radiological hazards due to naturally occurring radionuclides in the selected building materials used for the construction of dwellings in four districts of the Punjab province, Pakistan. *Radiat Prot Dosim* 153(3):352–360
- Righi S, and Bruzzi L. 2006. Natural radioactivity and radon exhalation in building materials used in Italian dwellings. *J Environ Radioact* 88:158–70. <https://doi.org/10.1016/j.jenvrad.2006.01.009>
- RPA. 2000. Naturally occurring radiation in the Nordic countries e Recommendations (The Flag e Book series) (Reykjavik). The Radiation Protection Authorities in Denmark, Finland, Iceland, Norway and Sweden
- Sahu SK, Tiwari M, Bhangare RC, and Pandit GG. 2014. Enrichment and particle size dependence of polonium and other naturally occurring radionuclides in coal ash. *J Environ Radioact* 138:421–426
- Sharma N, Singh J, Esakki SC, *et al.* 2015. A study of the natural radioactivity and radon exhalation rate in some cements used in India and its radiological significance. *J Radiat Res Appl Sci* 9(1):47–56
- Taskin H, Karavus M, Ay P, *et al.* 2009. Radionuclide concentrations in soil and life time cancer risk due to gamma radioactivity in Kirklareli, Turkey. *J Environ Radioact* 100:49–53. <https://doi.org/10.1016/j.jenvrad.2008.10.012>
- Trimble CA. 1968. Absolute counting of alpha decay and the radioactivity in water from hot spring National Park. Thesis. University of Arkansas
- Tsoufanidis N. 1995. Measurement and Detection of Radiation. Taylor and Francis, UK
- Tufail M, Nasim A, Sabiha J, *et al.* 2007. Natural radioactivity hazards of building bricks fabricated from soil of two districts of Pakistan. *J Radiological Prot* 27:481e492
- Tzortzis M, and Tsertos H. 2004. Determination of thorium, uranium and potassium Elemental concentrations in surface soils in Cyprus. *J Environ Radioact* 77:325–38. <https://doi.org/10.1016/j.jenvrad.2004.03.014>
- UNSCEAR (United Nations Scientific Committee on the Effects of Atomic Radiation). 1993. Sources and effects of Ionizing Radiation. Report to the General Assembly with annexes. United Nations, New York
- United Nations Scientific Committee on the effects of Atomic Radiation, UNSCEAR. 2000. Sources, effect and risks of ionising radiation. Report to the General Assembly with Scientific Annexes. United Nations. New York
- UNSCEAR. 1988a. Report of the United Nations Scientific Committee on the Effects of Atomic Radiation, United Nations. 647
- UNSCEAR. 1988b. Sources, effects and risks of ionizing radiation, Annex B, United Nations, New York
- Usikalu MR, Anoka OC, and Balogun FA. 2011. Radioactivity measurements of the Jos Tin mine tailing in Northern Nigeria. *Archives Phy Res* 2(2):80–86
- Usikalu MR, Fuwape IA, Jatto SS, *et al.* 2017. Assessment of radiological parameters of soil in Kogi State, Nigeria. *Environ Forensics* 18(1):1–14. doi:10.1080/15275922.2016.1263898
- World Health Organization. 2009. WHO Handbook on Indoor Radon: A Public Health Perspective. World Health Organization. WHO Press, Geneva, Switzerland
- Xinwei L. 2005. Natural radioactivity in some building materials of Xi'an, China. *Radiat Meas* 40(1):94–97
- Xinwei L, and Xiaolon Z. 2008. Natural radioactivity measurements in rock samples of Chihua Mountain National Geological Park, China. *Radiat Prot Dosim* 128:77–82